EUROPEAN ORGANIZATION FOR NUCLEAR RESEARCH

CERN-SPSC-2005-033
SPSC-M-741
12 September 2005

Status of DIRAC and DIRAC Addendum

The DIRAC Collaboration

[a] CERN, Geneva, Switzerland
[b] Czech Technical University, Prague, Czech Republic
[c] Institute of Physics ASCR, Prague, Czech Republic
[d] Ioannina University, Greece
[e] INFN - Laboratori Nazionali di Frascati, Frascati, Italy
[f] Trieste University and INFN-Trieste, Italy
[g] KEK, Tsukuba, Japan
[h] Kyoto Sangyou University, Japan
[i] UOEH-Kyushu, Japan
[j] Tokyo Metropolitan University, Japan
[k] National Institute for Physics and Nuclear Engineering IFIN-HH, Bucharest, Romania
[l] JINR Dubna, Russia
[m] IHEP Protvino, Russia
[n] Skobeltsyn Institute for Nuclear Physics of Moscow State University
[o] Santiago de Compostela University, Spain
[p] Basel University, Switzerland
[q] Bern University, Switzerland
[r] Zürich University, Switzerland

Spokesman: L.Nemenov,
e-mail: Leonid.Nemenov@cern.ch, tel.:+41-22-7673044, fax: +41-22-7679475

Contents

1 Status of DIRAC

In 2004–2005 offline analysis was focused on data taken during 1999-2003 runs. Based on the analysis of $\pi^+\pi^-$ pairs taken on a Ni target in 2001 the DIRAC Collaboration reported the observation of a first high statistics atomic data sample: 6530 ± 294 of atomic pairs above 374022 ± 3969 Coulomb-correlated background events [5]. Further analysis resulted in the first measurement of the $\pi^+\pi^-$ atom lifetime [6].

The break-up probability was found to be

$$P_{br} = 0.452 \pm 0.023_{stat}\ ^{+0.009}_{-0.032\}syst} = 0.452\ ^{+0.025}_{-0.039}. \quad (1)$$

The main systematic errors are due to

Quantitative determination of CC-background	± 0.007
Details of the signal shape	± 0.002
Multiple scattering	$+0.006/-0.013$
K^+K^- and $\bar{p}p$ admixtures	$+0.000/-0.023$
Finite size effects in CC background	$+0.000/-0.017$
Total	$+0.009/-0.032$

The result for the lifetime is

$$\tau_{1S} = \left[2.91\ ^{+0.45}_{-0.38\}stat}\ ^{+0.19}_{-0.49\}syst}\right] \times 10^{-15}\ \text{s} = \left[2.91\ ^{+0.49}_{-0.62}\right] \times 10^{-15}\ \text{s}. \quad (2)$$

Standard Chiral Perturbation Theory (SChPT) predicts $\tau_{1S} = (2.9 \pm 0.1) \times 10^{-15}$ s [7].

The measured lifetime corresponds to the difference of the S-wave $\pi\pi$ scattering lengths $|a_0 - a_2| = 0.264\ ^{+0.033}_{-0.020}\ m_\pi^{-1}$.

The accuracy achieved for the lifetime is about $+17\%$, almost entirely due to statistics and -21%, due to statistics and systematics in roughly equal parts. With full statistics the statistical errors may be reduced accordingly:

Number of Atomic pairs (approx.)

	1999	2000		2001		2002		2003	Sum
Target	Pt	Ni	Ti	Ti	Ni	Ni	Ni	Ni	
Beam (GeV/c)	24	24	24	24	24	20	24	20	
Sharp selection	280	1300	900	1500	**6500**	2000	2600	1500	**16600**
Downstream only									**27000**

In parallel to the analysis with full statistics systematical errors were also constrained. With a dedicated set-up in 2003 we measured the multiple scattering in our targets and all materials (detectors, windows) along the pion path in DIRAC spectrometer with 1% precision [8]. Further reduction of systematical errors is envisaged in future DIRAC program in 2006/2008:

CC-background	no improvement	± 0.007
Signal shape	no improvement	± 0.002
Multiple scattering	measured to $\pm 1\%$	± 0.002
K^+K^- and $\bar{p}p$ admixtures	to be measured[1]	$+0.000/-0.023$
Finite size effects	to be measured[2]/improved calculations	$+0.000/-0.017$
Total		$+0.008/-0.030$

[1] to be measured in 2006/2008 with new PID

[2] to be measured in 2006/2008 with new trigger for identical particles at low Q

Data quality was improved by fine tunings:

- Adjustments of drift characteristics almost run-by-run;
- Magnetic field adjustment and alignment tuning with Λ-mass.

A new preselection was done with these improvements will allow to analyse/reanalyse the whole data sample in the near future.

Another opportunity is to use only downstream detectors (Drift chambers) for tracking and to investigate only Q_L distribution which is less sensitive to multiple scattering and to the signal shape. Studies are under way.

2 DIRAC Addendum

2.1 Modified DIRAC setup

For the continuation of $A_{2\pi}$ lifetime measurement and for observation and lifetime measurement of $A_{\pi K}$ we have to upgrade the DIRAC experimental setup [4] retaining symmetric geometry (Fig. 1). In the symmetric geometry we will detect simultaneously πK "atomic" pairs of both signs with acceptable efficiency. In the following we present status and time scale of the modifications proposed in the Addendum to the DIRAC proposal [3]. The modified experimental setup is shown in Fig. 2.

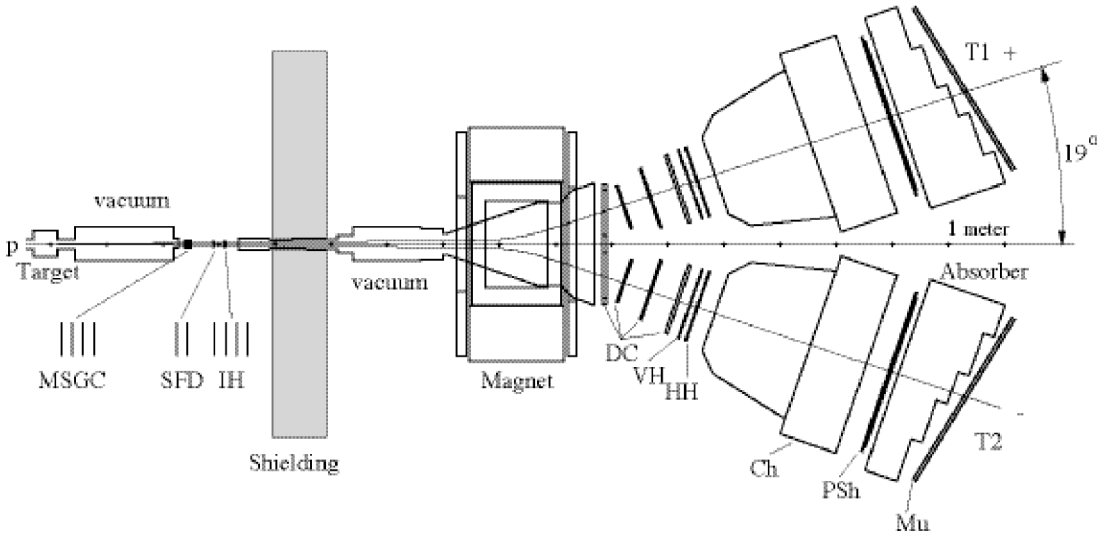

Figure 1: *Schematic top view of the DIRAC spectrometer. Upstream of the spectrometer magnet: microstrip gas chambers (MSGC), scintillating fiber detectors (SFD), ionization hodoscopes (IH). Downstream of the magnet, in each arm of the spectrometer: drift chambers (DC), vertical and horizontal scintillation hodoscopes (VH, HH), gas Cherenkov counters (Ch), preshower detector (PSh) and, behind the iron absorber, muon detector (Mu).*

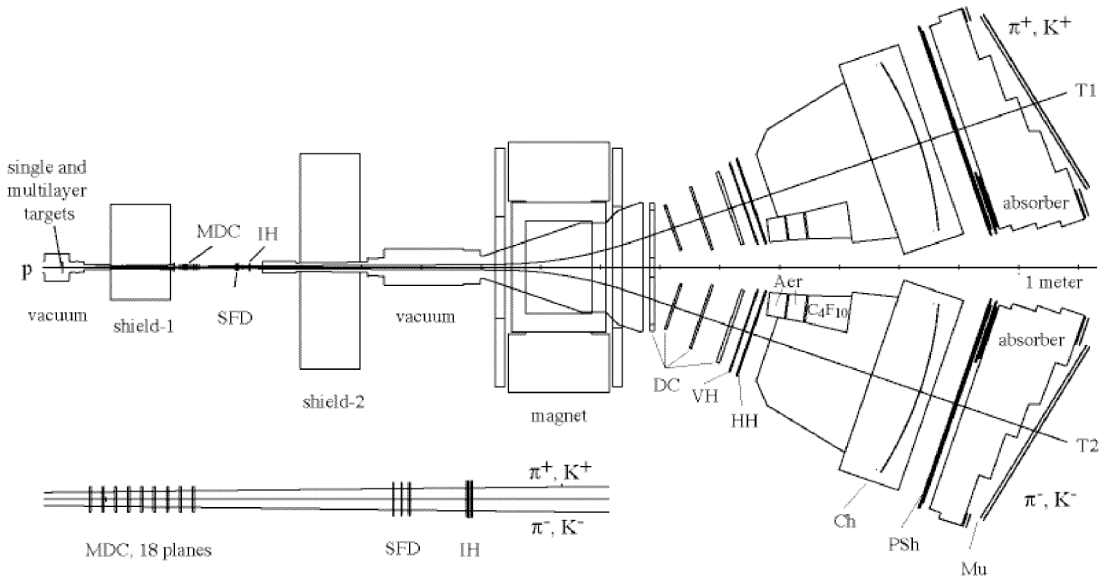

Figure 2: *Schematic top view of the upgraded DIRAC spectrometer. Upstream of the spectrometer magnet: microdrift chambers (MDC), scintillating fiber detectors (SFD), ionization hodoscopes (IH). Downstream of the magnet, in each arm of the spectrometer: drift chambers (DC), vertical and horizontal scintillation hodoscopes (VH, HH), aerogel Cherenkov counters (Aer). gas Cherenkov counters with N_2 (Ch) and heavy gas (C4F10), preshower detector (PSh) and, behind the iron absorber, muon detector (Mu).*

2.2 Channel and shielding

New vacuum section with collimators for the primary and secondary beams (fig. 3) will be manufactured by the middle of October 2005, transported from Dubna to CERN by the end of this year and installed together with iron shielding (fig. 4) into the DIRAC setup in the first quarter of the next year.

There will be a possibility for the installation of a permanent magnet and a thin foil of Pt into the secondary beam part of the new vacuum section in order to observe $A_{2\pi}$ long-lived nP states. Measurement of the $A_{2\pi}$ yield with and without B-field would allow to measure the

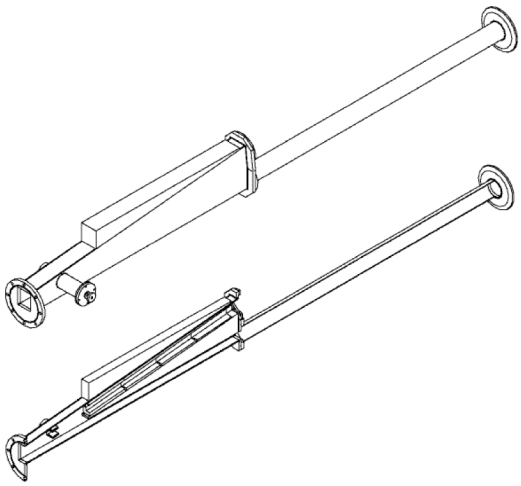

Figure 3: *New vacuum section.*

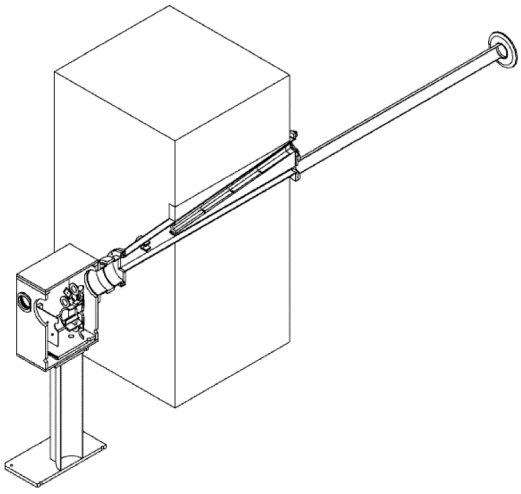

Figure 4: *Target station, bellows, new vacuum section and new shielding sliced along the proton beam.*

energy splitting $\Delta E(nS - nP)$ and the combination of the $\pi\pi$ scattering lengths $2a_0 + a_2$.

2.3 Microdrift Chambers (MDC)

During the last four years the MDC detector was designed, constructed and tested under experimental conditions. The most important features of the detector are:

- spatial accuracy < 30 μm (22 ± 4 μm from the beam test);
- double track resolution < 200 μm;
- one plane efficiency at the beam intensity $I = 2 \times 10^{11}$ protons per spill $> 98\%$ ($> 99\%$ from the beam test);
- low multiple scattering: total detector thickness $< 5 \times 10^{-3}$ X_0;
- drift time < 30 ns;
- time resolution < 1 ns;
- low readout time < 3 μs.

According to the results of MDC tests in 2003-2004, the detector stability has to be improved for the DIRAC heavy radiation conditions. This improvement will be achieved by some modification of MDC electrodes. It is planned to make new electrodes at JINR during February-April 2006. The modified MDC detector will be tested with a radioactive source for high voltage in April-May 2006.

DIRAC beam time is scheduled for July-September 2006. Before this period, i.e. in June 2006, the MDC detector will be mounted in the DIRAC setup at CERN.

2.4 Scintillation Fiber Detector (SFD)

A new SFD will be used (instead of existing X- and Y-planes) to improve space resolution and efficiency for adjacent double-hit detection. The new SFD may be used as a very efficient trigger device especially with a permanent magnet placed after the target; the test is planned. The U-plane will be used as it is, except for a modification of the PSC read-out algorithm, which leads to a better efficiency for adjacent hits. [1]

New SFD expected parameters

Number of planes	2
Distance from the target	3 m
Size of the plane	100×100 mm^2
Number of SciFi columns per plane	8
Thickness of the material for one plane:	3 mm (1% RL)
Fiber light guide length	350 mm
Mean light output	≈ 11 p.e.
Mean Det. Efficiency	$\approx 98\%$
Time Resolution without coordinate and amplitude corrections	≈ 0.46 ns
Space resolution	60 μm

[1] PSC read-out has a significant drawback for correlated adjacent double-hit detection efficiency (30% loss). The detection efficiency will be significantly recovered with the modified algorithm (5-10% loss).

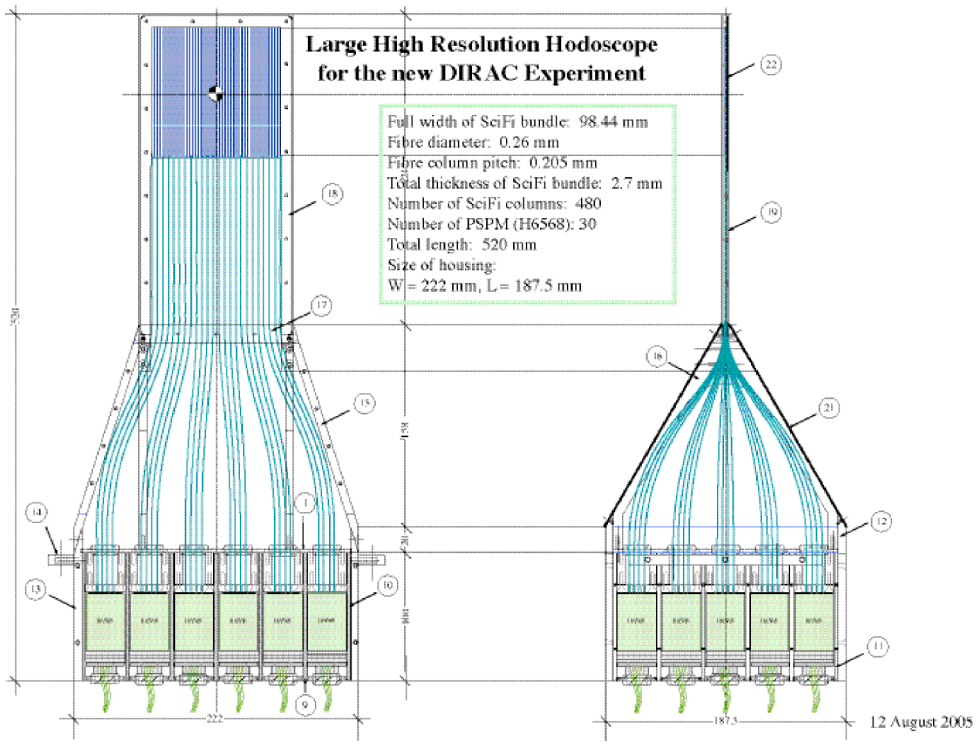

Figure 5: *Side views of one plane of the new SFD.*

The current solution for front-end (FE) electronics is ordinary discriminator with fixed threshold (as it was realized for the F1 Prototype in 2004). This scheme eliminates the problem of adjacent double hits that occurred with the PSC. It leads, however, to an increase of multiplicity for single hit detection of about 25%, for double hits of 50% with respect to the electronics with PSC. Additional read-out to ADCs allows for multiplicity suppression off-line.

Two prototypes 50×50 mm^2 of the new SFD with spatial resolution 60 μm were manufactured and tested in beam in summer 2004.

Additional tests of the F1 Prototype with a radioactive source are scheduled for October 2005. Production of fiber layers and detector housing will be finished in December 2005. Components for FE electronics will be delivered in two steps: 480 channels before the end of 2005 and 480 channels before March 2006. All electronics boards will be finished by May 2006. The full detector will be assembled before the beam test at T8 scheduled for June 2006.

2.5 Ionisation Hodoscope

In 2006 the detector will be used without changes [9].

2.6 Drift Chambers

The drift chambers are used to perform particle tracking after the magnet. The DC system consists of four chamber modules per arm including 6 sensitive planes in X and Y projection.

The first module (DC1) has a frame common to both arms; it has two active regions of 80×40 cm^2 housing 6 planes of signal wires (X, Y, W, X', Y', W').

Three modules are placed in each spectrometer arm:

- DC2 with an active area of 80×40 cm^2 and 2 wire planes (X, Y);
- DC3 with an active area of 112×40 cm^2 and 2 wire planes (X, Y);
- DC4 with an active area of 128×40 cm^2 and 4 wire planes (X, Y, X', Y').

Altogether the DC system consists of 11 modules, including spare ones.

After successful and long drift chamber operation at the first stage of the experiment, it was decided to perform full revision of all drift chambers. In the first half of 2004, seven modules (one DC1, three DC2, two DC3 and one DC4) were overhauled. In October-November one more DC4 module will be treated. At the same time all these modules will be tested with radioactive source. So, all DC modules to be installed in the DIRAC setup will be ready by the end of 2005. In the first half of 2006 all remaining spare DC modules will be overhauled.

2.7 Vertical Hodoscopes

Four slabs (two slabs per arm) will be added to the existing vertical scintillation hodoscopes (fig. 6). Each slab is $400 \times 70 \times 20$ mm^3 $(L \times W \times T)$. These slabs will be manufactured in the first quarter 2006.

2.8 Horizontal Hodoscopes

New longer horizontal hodoscopes will be installed instead of the existing ones (fig. 7). There will be 32 slabs (16 slabs per arm) by $1500 \times 25 \times 25$ mm^3 $(L \times W \times T)$. Photomultipliers for the horizontal hodoscopes are already at CERN. Scintillators will be transported to CERN at the end of September 2005. The hodoscopes will be assembled at the end of November 2005.

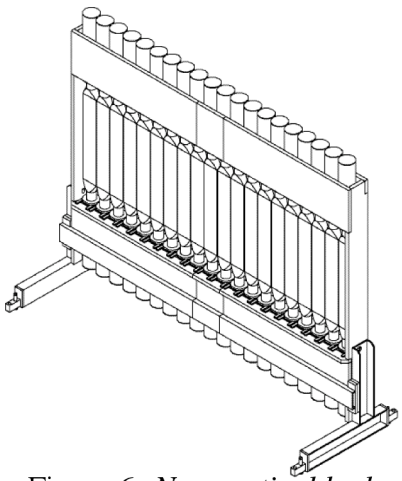

Figure 6: *New vertical hodoscope.*

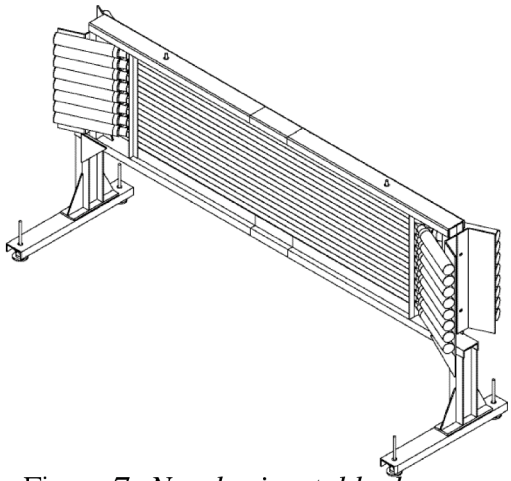

Figure 7: *New horizontal hodoscope.*

2.9 Aerogel Cherenkov detectors

The πK part of the experiment requires $p,\ K,\ \pi,\ e$ separation. The new C_4F_{10} gas Čerenkov counter discriminates K from π, while the aerogel Čerenkov counter discriminates p from K. Contaminating protons in the left arm (and to a lesser extent antiprotons in the right arm) are

suppressed since they are below threshold for Čerenkov radiation. Kaons from $K\pi$ atoms have momenta between 3.9 and 8.9 GeV/c. We will need 2, possibly 3, indices of refraction to detect kaons while suppressing protons. Hence we plan to build 3 aerogel counters in the π^+K^- and π^-K^+ arms each viewed by 2 photomultipliers. The aerogel thickness will be 15 cm and the vertical length 40 cm, determined by acceptance (fig. 8).

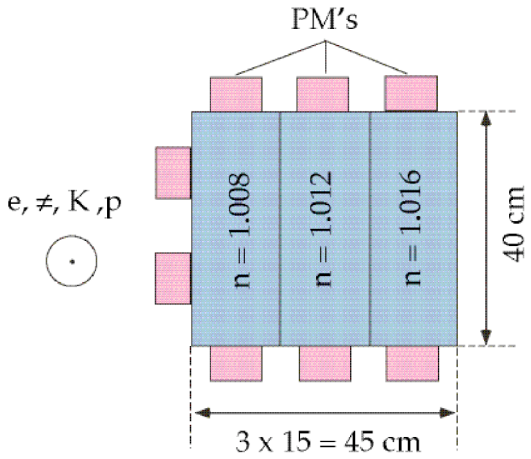

Figure 8: *Sketch of the aerogel setup. Small angles with respect to the primary proton beam are towards the left. Two additional photomultipliers mounted on the side will compensate for the low light yield at small angles.*

We have measured the light yield of aerogel and optimized the geometry. Most of the measurements were made with $n = 1.05$ aerogel from the Budker Institute of Nuclear Physics in Novosibirsk. We have measured the number N_{pe} of photoelectrons (p.e.) as a function of thickness for a 10 cm long slab of 1.05 aerogel viewed by two photomultipliers (5" Hamamatsu 1584 bialkali with UV window, 25% quantum efficiency between 200 and 450 nm). The measurements were made with cosmic ray muons which have an average momentum of 700 MeV/c. A novel setup using wavelength shifters (WLS) gives promising results (fig. 9, left). The 2.5 cm thick aerogel tiles are sandwiched between reflective tetratex foils which are sprayed with WLS. For example, p-Terphenyl dissolved e.g. in chloroform shifts light from 270 to 340 nm, which reduces absorption and leads to some 5.5 p.e./cm. Scaling to 15 cm of the $n = 1.008$ aerogel, we expect $4 - 15$ photoelectrons for kaons between 4.5 and 9 GeV/c. These yields need to

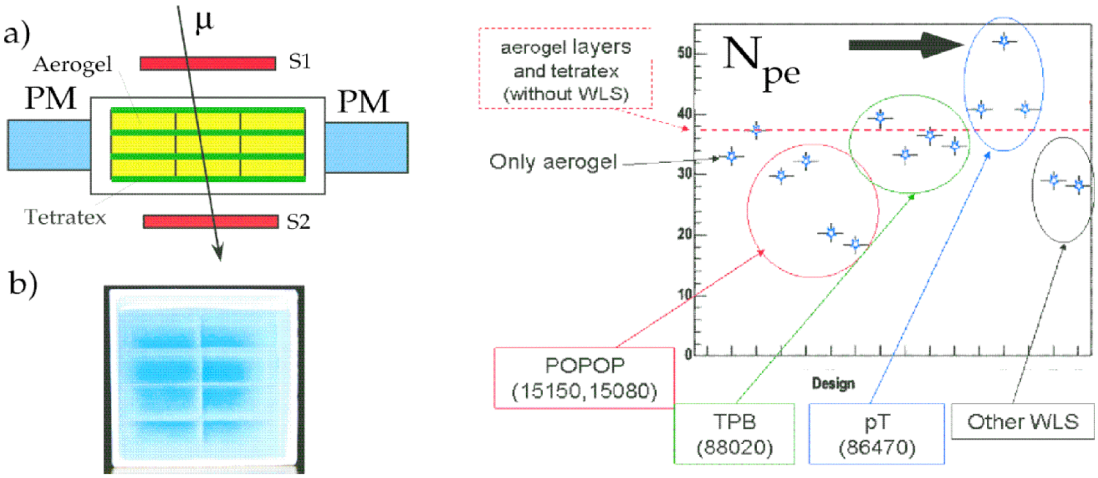

Figure 9: *Left: a) setup for light yield measurements, b) photograph of the aerogel tiles. Right: number of photoelectrons for 10 cm $n = 1.05$ aerogel, using cosmic muons ($\bar{\beta} = 0.989$), and for different geometries and WLS. The arrow shows the optimum design with p-Terphenyl dissolved in chloroform.*

be checked (due e.g. to absorption losses) with a prototype of the final length and depth. The $n = 1.008$ aerogel has been ordered. A prototype made of 7 liters of the $n = 1.008$ aerogel will be available for tests in January 2006. The installation of the detectors in the experimental area is planned at the end of June 2006, before data taking resumes with DIRAC.

2.10 Cherenkov detectors (C_4F_{10} and N_2)

For the detection of $A_{2\pi}$, $A_{\pi^+K^-}$ and $A_{\pi^-K^+}$ we have to separate electrons, pions and kaons in the right arm, and positrons, pions, kaons and protons in the left arm of the spectrometer.

To suppress electrons and positrons we will use the existing gas Cherenkov counters filled with nitrogen (N_2). But these counters have to be modified to provide space for heavy gas Cherenkov counters needed for pion-kaon separation. The decrease of the detection volume will lower the electron rejection efficiency. This efficiency loss will, however, be compensated by a modification of the Preshower detector.

For π and K separation we will use new gas Cherenkov counters filled with C_4F_{10} ($n = 1.0014$). Perfluorobutane under normal atmospheric conditions is a nontoxic, nonflammable, chemically inert, noncorrosive gas. A gas system with circulation and cleaning will be used.

The dimensions of the new gas Cherenkov counters were obtained by simulation and tracking of pions and kaons from $A_{\pi K}$ breakup through the magnetic field. Events were selected if both π and K were detected by all drift chambers. In fig. 10 the "particle box" is shown which is limited in space by the HHs and the mirrors of the existing Cherenkov, and covers the momentum range between 4 and 11 GeV/c. This "particle box" includes all the kaons from $A_{\pi K}$ atoms. Divergency angles of the box in the horizontal and vertical planes are $6.2°$ and $2°$, respectively. The box length is 280 cm.

The "particle box" contains 2 layers of aerogel counters (30+30 cm), the new Cherenkov gas counter filled with C_4F_{10} (65 cm, 10 p.e. from 4 GeV/c pions), part of the existing Cherenkov with N_2 (144 cm, 8.5 p.e. from electrons) and four gaps between detectors (11 cm). The performance of the existing Cherenkov (15 p.e. per 253 cm of N_2) was used to estimate $n_{p.e.}$ in C_4F_{10}.

The "light box" (fig. 11) for the C_4F_{10} counter should be wider than the "particle box" because of the Cherenkov radiation angle for electrons ($\theta = 3.03°$).

For the simulation of Cherenkov light from electrons in the C_4F_{10} counter the "particle box" was divided into four parts because we intend to use 4 PMs per counter. Because of the mirror symmetry it is enough to simulate 1/8th of the counter.

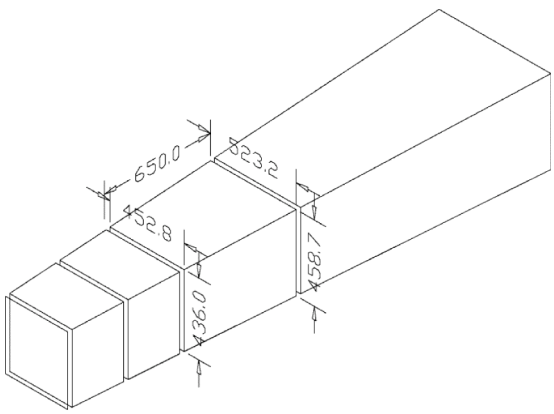

Figure 10: *"Particle boxes": two aerogel, C_4F_{10} and N_2 counters.*

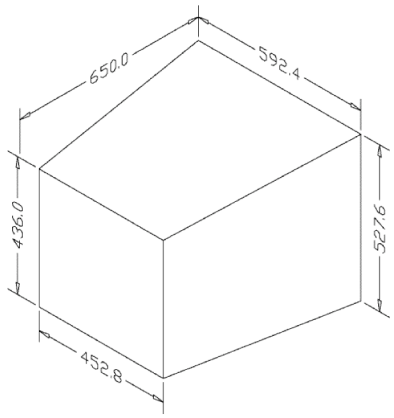

Figure 11: *"Light box" for C_4F_{10} counter.*

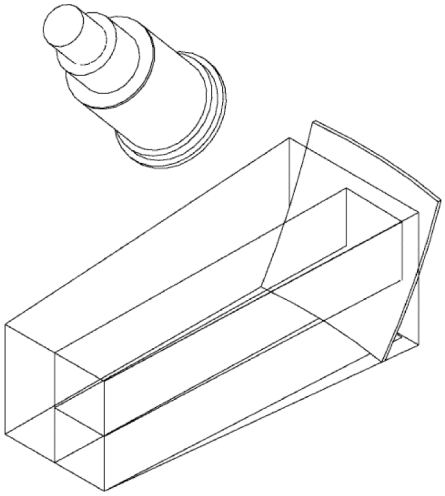

Figure 12: *Mirror after cutting by 1/4 of the "light box".*

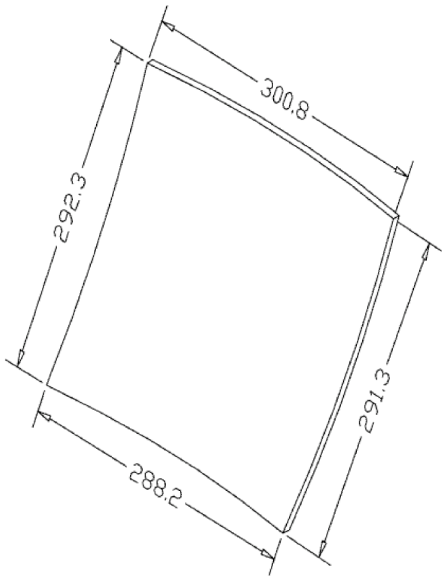

Figure 13: *Dimensions of the mirror.*

The radius of curvature of the mirror is 1194 mm as in the existing Cherenkov. The mirror and PM were rotated in the vertical plane by 25° and 50°, respectively. In this geometry the PM housing is flush with the front side of the "particle box". The photocathode diameter is 125 mm. The distance from PM photocathode to the back side of the "particle (light) box" is 630 mm, slightly longer than the focus distance because of the particle beam divergency. The mirror was cut by 1/4 of the "light box" (fig. 12). The mirror dimensions are shown in fig. 13.

Cherenkov light from electrons was reflected by the mirror and Cherenkov rings were drawn on the PM photocathode (fig. 14). It is clear that the Cherenkov light focusing is good. Four mirrors and four photocathodes are shown in fig. 15. The Cherenkov counter is shown in fig. 16.

Design of the detector will be ready by November 2005. In October request for mirrors production will be prepared. Final drawings of the detector support and housing will be ready in January 2006. Production will take 3 months and will be finished by May 2006. Detector with mirrors and gas system will be assembled in May-June 2006.

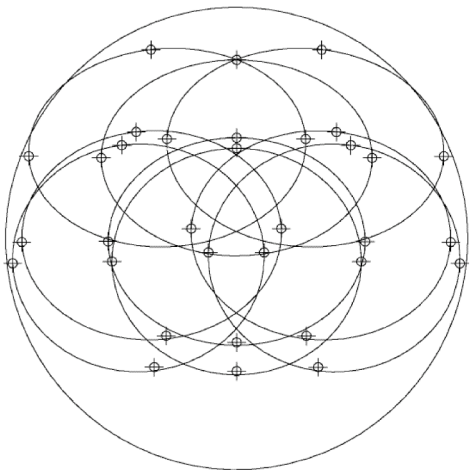

Figure 14: *Cherenkov rings from electrons on the photocathode.*

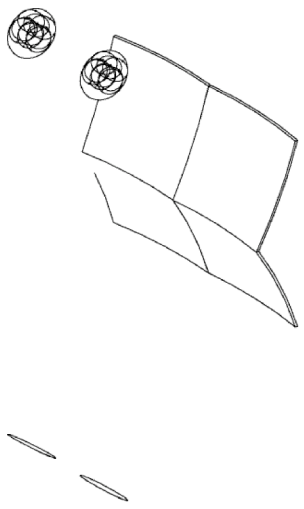

Figure 15: *Isometric view of the mirrors and photocathodes.*

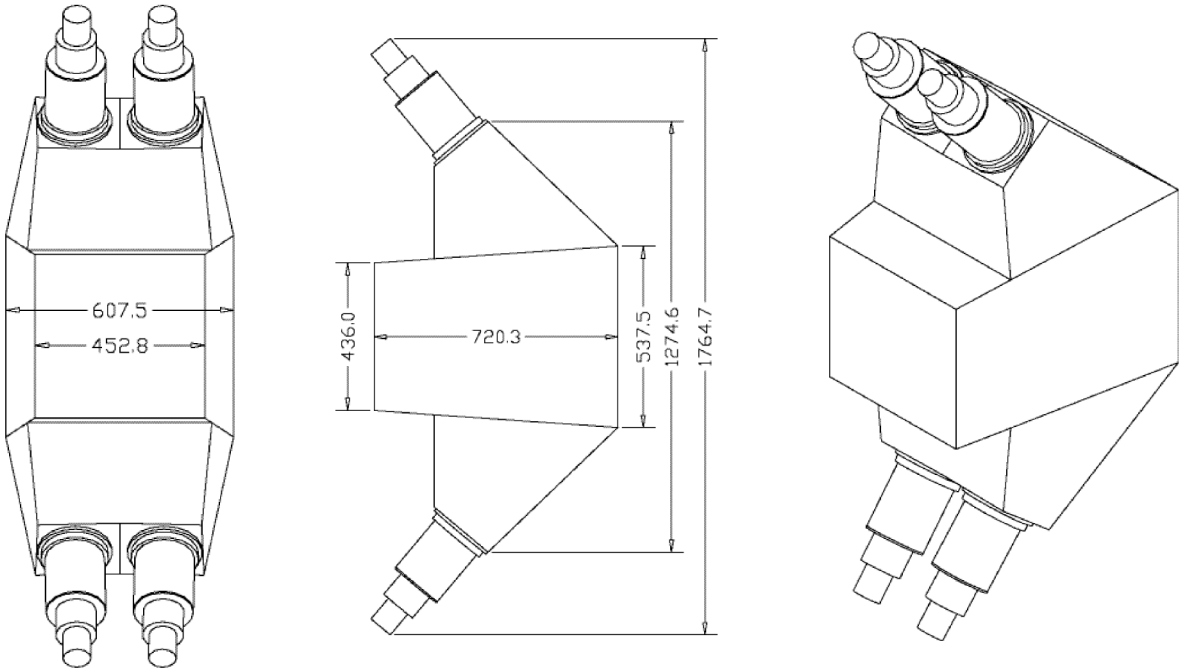

Figure 16: *Front, side and isometric views of the heavy gas Cherenkov counter.*

2.11 Preshower detectors

The Preshower Detector upgrade refer to the acceptance enhancement, with a larger geometry and momentum space for particle detection. Moreover, the new heavy gas Cherenkov detectors for $\pi - K$ separation, will be placed within the existing Nitrogen Cherenkov detector. Therefore, by decreasing the detection volume, the electron rejection efficiency of the Cherenkov detector, will be lower. To compensate this, the Preshower Detector rejection efficiency must be increased. According to our studies [10], the best preshower configuration must use (see Fig. 17) a maximum of $6X_0$ overall Pb thickness, which provides an *electron rejection* $\geq 95\%$ with a *pion efficiency* $\geq 90\%$. This can be subdivided in two layers, with 2-3X_0 thick each. So, a possible rejection inefficiency of one layer can be compensated by the other one, and the multilayer configuration can improve the overall *electron rejection*.

For this aim we realized a two layer Preshower Detector, for each arm. The new configuration can be seen in Fig. 18

The new components of the Preshower Detector will be at CERN in the beginning of October 2005. They include

- 2 frames for two layers (large + small)
- 34 new scintillators BC-408 (750mm x 175mm x 10mm)
- 6 Pb converters (850mm x 350mm x 25mm)
- 8 Pb converters (850mm x 350mm x 10mm)

The IFIN-HH Bucharest team will come to CERN around of 15 October 2005 to prepare new detectors, to dismount the old preshower and to mount the new one.

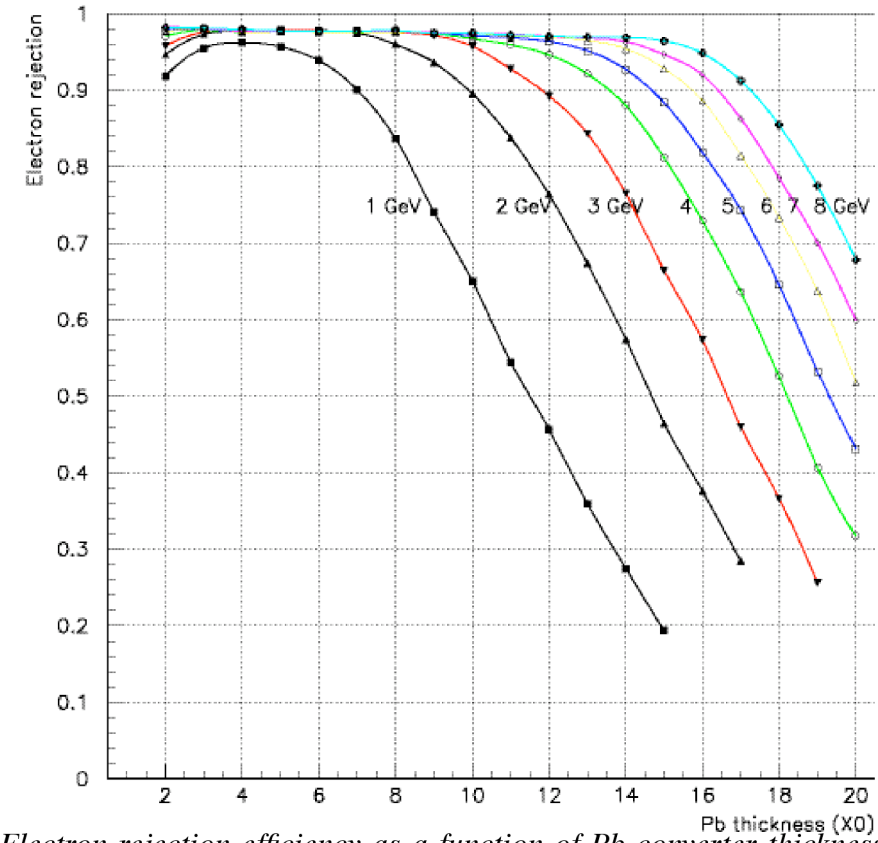

Figure 17: *Electron rejection efficiency as a function of Pb converter thickness (in radiation lengths X_0 units), for $1 - 8$ GeV incident electrons.*

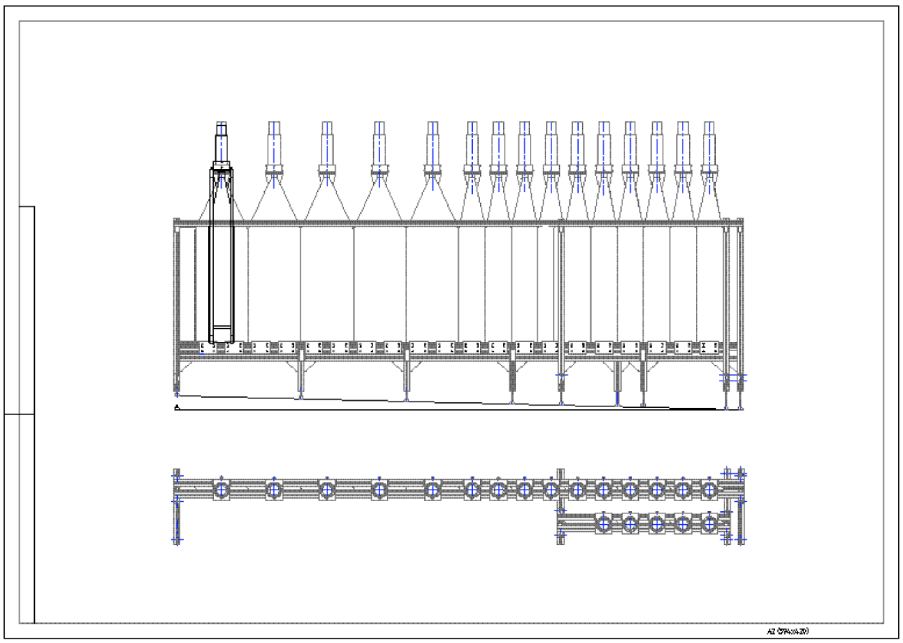

Figure 18: *Mechanical design of the new Preshower Detector.*

2.12 Muon detectors

12 slabs (6 slabs per arm) will be added to the existing muon scintillation hodoscopes in order to increase its acceptance (fig. 19). Muons are essentially rejected by the existing detector,

and the additions improve the efficiernсy by a few percent only.The new slabs will be installed in 2007.

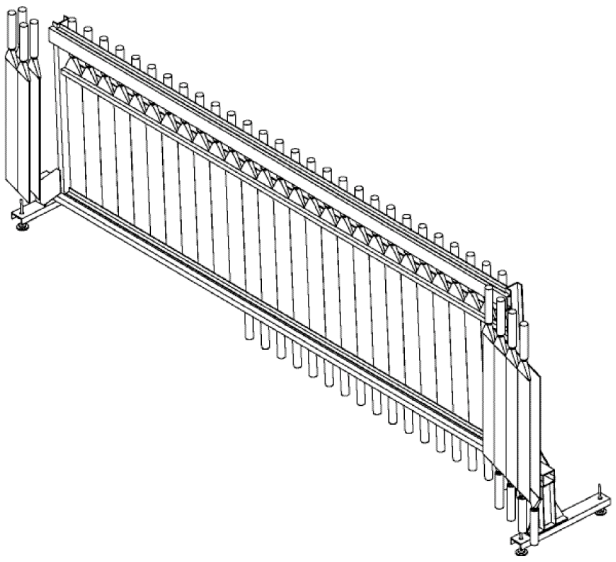

Figure 19: *Modified Muon detector.*

2.13 Readout system

In 2006 new electronics developed by V. Karpukhin will be used with SciFi detector, where it was tested so far. This electronics uses a high-speed USB bus for data transfer (see fig. 20). In 2004 a prototype D412(ADC+TDC) which is based on F1 chip was successfully tested with 32 channels of SFD. The level translator to LVDS and pulse width shaper modules have been developed, and a transmitter prototype will soon be ready. For the 2006 run, besides the SFD also the VH, HH, Aerogel and gas Cherenkov detectors will be equipped with the new read-out system.

2.14 Trigger

In 2006 the following trigger configuration is foreseen in DIRAC:

- Triggers for detection of $\pi^+\pi^-$ and $K^+\pi^-$ atoms. These triggers are arranged as two-level systems with a fast first level trigger and second level dedicated processors using drift chamber information.
- Trigger for $K^-\pi^+$ atoms. In 2006 it will be a single-level trigger. In 2007 a new processor will be implemented for better event selection with two-level system like in the previous item.
- Other triggers for physics and calibrations which will detect:

  K^+K^- pairs

  $p\bar{p}$ pairs

  $\pi^-\pi^-$ pairs

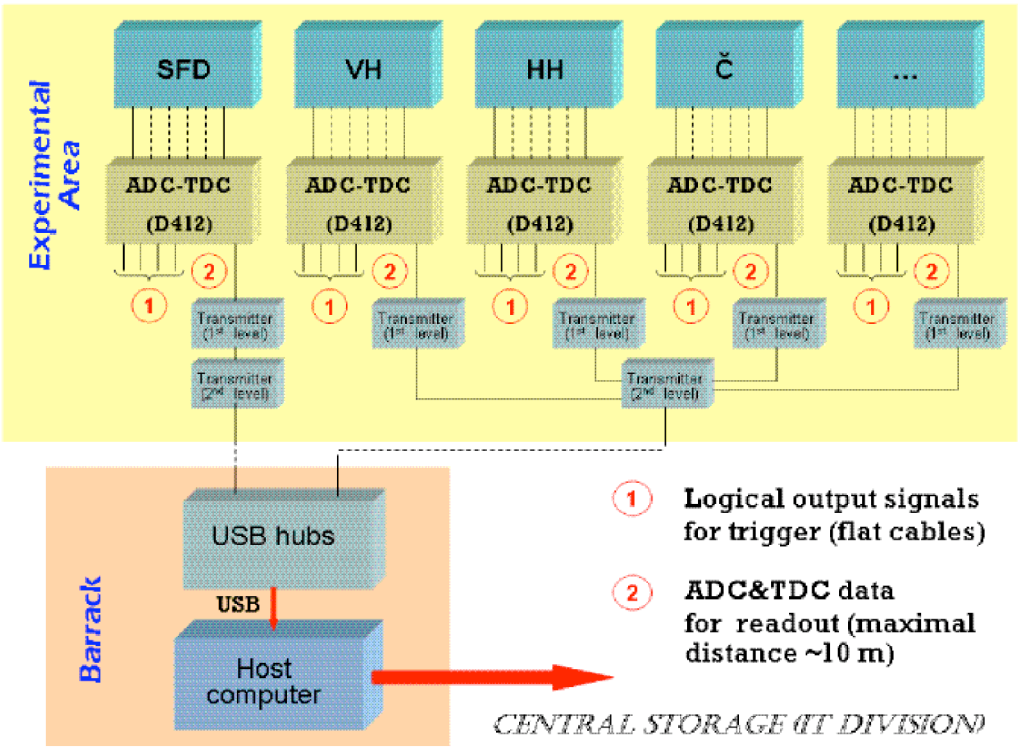

Figure 20: *Schematic layout of DIRAC Readout*

e^+e^- pairs

Λ-decays to $p\pi^-$

double e^+e^- pairs.

Other triggers for the setup tuning will be provided as well.

The trigger system with the above features will be ready when beam starts and tuned in the initial part of the DIRAC 2006 run.

2.15 DAQ

The schematic layout of the existing DIRAC data acquisition system is shown in figure 21. The main feature of DIRAC DAQ [11] is that all data from subdetectors coming in during the accelerator burst are transferred to VME buffer memory modules or stored in dedicated electronic modules without any software intervention. Relatively slow operations like read-out, hardware checks etc. are performed during a pause between bursts and hence the maximal operation rate of DAQ electronics is provided. An event building is implemented as a separate layer, and this layer is running on the main DAQ host.

A separate event building layer gives several advantages:

1. Reduced requirements for VME processor resources and for links which are used for sending data to main DAQ host.

2. Increased scalability (with separate event building one can use several VME processors and other data sources).

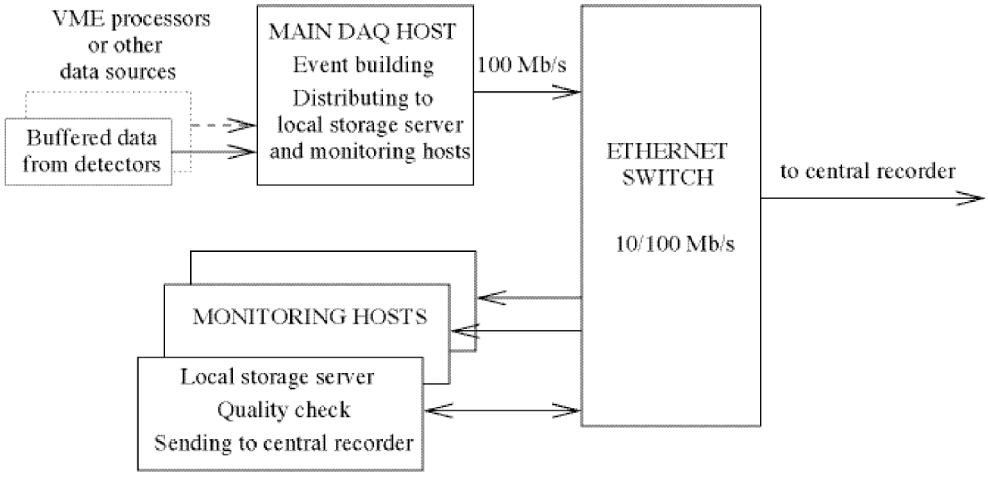

Figure 21: *Schematic layout of DIRAC DAQ*

3. Simplified programming of hardware specific readout.

In the extension of the experiment, we will have an increase in both the number of events per cycle and in the event size (these are due to higher intensity and new detectors).

- **Number of events**
  According to [3] the total efficiency will be increased by a factor of 4 (4k events/spill for standard runs).

- **Event size**
  By realistic estimations the average event size will increase by a factor of 2 (from 1 KB to 2 KB). Some reserve is desirable, therefore a safer estimate is 4 KB/event.

It is also expected that we will work with 2..3 cycles per supercycle and that a supercycle will have a duration of about 17 seconds. The expected PS supercycle structure is shown in figure 22. Number 2..3 means that DAQ should be prepared for working with at least 3 cycles/supercycle.

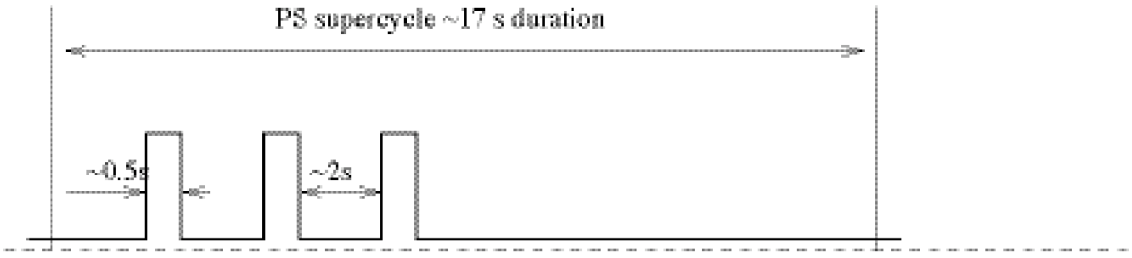

Figure 22: *PS super-cycle as seen by DIRAC setup*

So we will have:

- with realistic estimation:
  8 MB/cycle 24 MB/supercycle 120 GB/day

- with safe estimation:
  16 MB/cycle 48 MB/supercycle 240 GB/day

It is also planned that some detectors will migrate to new electronics developed by V. Karpukhin. This electronics will use high-speed USB bus for data transfer. Scintillation fiber detector (SFD) is the first detector which will use USB-readout.

Our analysis leads to the conclusion that existing DIRAC data acquisition system is able to work for the extension of experiment, and relatively small changes are required for handling the increased data samples and new hardware. Required changes are discussed in [12].

The main efforts of DAQ team will be concentrated on the following tasks:

- Revising of DAQ software for finding and eliminating possible limitations (for example, on max. number of events, sizes of data blocks, and so on). This work is partly done, and will be finished during year 2005.
- Revising software for automatic and interactive on-line monitoring of data. This work will be done partly in spring 2006, and will be finished during test runs in summer 2006.
- Upgrading and tuning hardware and operating systems for computers which are critical for data acquisition system. This includes upgrading of main DAQ host and the on-line monitoring host (fall of 2005), and installing dedicated computer which will serve as a local disk storage and also will run quality check software (spring-summer of year 2006).
- Writing software for handling new electronic modules developed by V.Karpukhin. We expect that prototypes of these modules will be available at the beginning of year 2006, and plan to finish writing software for them in April-May of 2006.

References

[1] B. Adeva, *et al.*, CERN/SPSLC 95–1, SPSLC/P 284, Geneva 1995; http://cern.ch/dirac.

[2] B. Adeva, *et al.*, CERN-SPSC-2000-032, CERN-SPSC-P-284-ADD-1 (2000) 74pp.

[3] B. Adeva, *et al.*, CERN-SPSC-2004-009, CERN-SPSC-P-284-ADD-4 (2004) 168pp.

[4] B. Adeva, *et al.*, Nucl. Instrum. Meth. A515 (2003) 467-49.

[5] B. Adeva, *et al.*, J. Phys. G: Nucl. Part. Phys. 30 (2004) 1929-1946.

[6] B. Adeva, *et al.*, Phys. Lett. B619 (2005) 50-60.

[7] G. Colangelo, J. Gasser and H. Leutwyler, Nucl. Phys. B603 (2001) 125.

[8] A. Dudarev, *et al.*, DIRAC intenal note 05-02.

[9] G. Bitsadze, *et al.*, Nucl. Instrum. Meth. A533 (2004) 353-360.

[10] M.Pentia, S.Constantinescu, C.Ciocarlan, to be published as DIRAC internal note.

[11] V. Olshevsky and S. Trusov, Nucl. Instrum. Meth. A469 (2001) 216.

[12] V. Olchevskii, DIRAC internal note 05-12.